Journal of Physics: Conference Series **527** (2014) 012025 doi:10.1088/1742-6596/527/1/012025

Nucleon tomography

Marco Radici

INFN - Sezione di Pavia, via Bassi 6, I-27100 Pavia, Italy

E-mail: marco.radici@pv.infn.it

Abstract. Starting from the interpretation of the nucleon electromagnetic form factors in terms of charge/magnetic density, we illustrate the need and the advantages of a multi-dimensional exploration of the structure of the nucleon, and in general of hadrons. We introduce new tools, like the Generalized Parton Distributions (GPDs) and the Transverse Momentum Distributions (TMDs), which enable us to explore the dynamics of partons beyond the usual collinear approximation adopted in the QCD analysis of hard processes. We emphasize the possibility of using these tools to address the (orbital) angular momentum of partons, and we highlight the latest results on the partonic decomposition of the nucleon spin. We briefly touch on the possible breaking of universality for a specific category of TMDs; as an example, we describe the Sivers effect as a fundamental test of our understanding of the color force in QCD.

1. Introduction

The nucleon is the most common element in the universe. It makes up 99.97% of visible matter. As a composite system of more elementary strongly-interacting constituents, the nucleon is difficult to be studied within QCD. In fact, its extension is of the order of femtometer; probing it requires an energy scale where α_s is large and QCD cannot be calculated with perturbative methods. We are not yet able to deduce from first principles how the nucleon structure comes about by displaying the confinement of strongly interacting quarks and gluons. At present, the most powerful attempt to solve QCD in nonperturbative regime is describing the theory on a lattice. But most of the nucleon's macroscopic properties (mass, spin, charge, magnetic moment, charge radius,..) cannot yet be explained. Let's consider for example the nucleon mass. The Higgs mechanism justifies the origin of mass of the elementary particles, like quarks, inside the Standard Model. But the mass of light quarks that determine the charge, baryon number, and isospin of the nucleon, amounts to about 1% of its total mass. What does it generate the missing 99%? QCD is a highly nonlinear theory. At the nucleon scale, its chiral symmetry is spontaneously broken; the vacuum has a nontrivial structure with nonvanishing quark and gluon condensates. Below the scale of chiral symmetry breaking, the light quarks rapidly acquire mass because of the interaction with gluon and sea-quark clouds. Therefore, almost all of the nucleon mass is given by the interaction energy involved in the QCD mechanisms that lead to confinement [1].

One of the ways to understand confinement is to study the internal structure of the nucleon, and in general of hadrons, in higher and higher detail. This requires the probe being more and more energetic. A typical tool is electron scattering in the Deep-Inelastic regime (DIS), where the 4-momentum q transferred to the target becomes larger and larger but keeping the ratio $x_B = Q^2/2P \cdot q$ fixed, with P the target 4-momentum and $Q^2 = -q^2$. The kinematics is

highly relativistic and it is useful to describe the system in terms of Light-Cone (LC) variables (a 4-vector a is represented as $a = \{a^+, a^-, \boldsymbol{a}_T\}$, with $a^\pm = (a^0 \pm a^3)/\sqrt{2}$). In fact, if the target is initially at rest, after absorbing the virtual photon it gets boosted along the direction of the spatial momentum transfer, say $\hat{z}$. Since $Q \to \infty$, the target momentum has a dominant component, $P^+ \sim Q$, while $P^- \sim 1/P^+$ is suppressed. The nucleon target gets squeezed to a disk along the boost direction by Lorentz transformations, and it can be conceived as an assembly of partons traveling collinearly with the parent nucleon, with LC "longitudinal" momenta $p^+ = xP^+$ and transverse momenta $|\boldsymbol{p}_T| \ll p^+$, with $x \sim x_B$.

In such a highly relativistic framework, conventionally named Infinite Momentum Frame (IMF), the usual textbook interpretation of the electromagnetic form factors of the nucleon as Fourier transforms of its charge and magnetization densities, is incorrect [2]. The main difficulty lies in the fact that the form factors are deduced from matrix elements where the initial and final nucleon states have different momenta, hence different wave functions. The Dirac and Pauli form factors parametrize the nucleon matrix elements of the electromagnetic current operator J^μ as

$$\langle N'(P',S')|\hat{J}^\mu(0)|N(P,S)\rangle = \bar{u}(N')\gamma^\mu u_N\, F_1(Q^2) + \bar{u}(N')i\frac{\sigma^{\mu\nu}q_\nu}{2M}u_N\, F_2(Q^2)\ . \tag{1}$$

It is useful to adopt the so-called Sachs form factors

$$G_E(Q^2) = F_1(Q^2) - \frac{Q^2}{4M^2}F_2(Q^2)\ , \quad G_M(Q^2) = F_1(Q^2) + F_2(Q^2)\ , \tag{2}$$

because the expression of the electron-nucleon cross section (in the one-photon approximation) depends directly on $G^2_{E/M}$ but not on $G_E G_M$. In the Breit frame where $\boldsymbol{q}/2 = \boldsymbol{P'} = -\boldsymbol{P}$ and $q^0 = 0$, G_E is simply given as the nucleon helicity-flip matrix element of $\hat{J}^0$. If the nucleon wave function could be expressed as the product of a plane wave, describing the motion of the center of mass (c.m.) with momentum $\boldsymbol{P}$, and of a function $\varphi(r)$ depending only on the internal relative coordinate r, then the Fourier transform of G_E

$$\rho(r) = \frac{2}{\pi}\int_0^\infty dQQ^2\, j_0(Qr)\, G_E(Q^2) \tag{3}$$

would be related to $\rho(r) = |\varphi(r)|^2$, i.e. to the charge density of the nucleon. However, the above relation holds only for a nonrelativistic system. For a relativistic system like the nucleon in the IMF, the Nakanishi integral representation of the Bethe-Salpeter wave function shows that the covariant wave function cannot be simply factorized in a part describing the c.m. motion and in another one describing the internal motion: it depends explicitly and intrinsically also on the total momentum $\boldsymbol{P}$. Therefore the initial and final nucleon wave functions in the Breit frame are different, and the Fourier transform of G_E cannot be interpreted as a quantum mechanical density, namely as the modulus squared of some function [3].

We are thus confronted with the problem of identifying the proper operator whose matrix elements give the nucleon electromagnetic form factors, but that at the same time it can be related to the diagonal matrix element of a density operator.

2. The Generalized Parton Distributions

The solution to the puzzle relies on the crucial observation that the electromagnetic form factors are extracted from nucleon matrix elements of a local current operator (see equation (1)). An elegant way out is to rewrite them involving the charge density operator in IMF, $\hat{J}^+$, and re-express them in terms of a nonlocal operator along the LC x^- direction (conjugated to the

dominant component P^+ in momentum space) [4, 5]:

$$\begin{aligned}\langle N'|J^+(0)|N\rangle &\equiv \langle N'|\overline{q}(0)\gamma^+ q(0)|N\rangle = \overline{u}_{N'}\gamma^+ u_N\, F_1(t) + \overline{u}_{N'}\frac{i\sigma^{+\nu}q_\nu}{2M}u_N\, F_2(t)\\ &\equiv \int dx \int \frac{dx^-}{2\pi}\, e^{ixP^+x^-}\, \langle N'|\overline{q}\Big(-\frac{x^-}{2},0,\mathbf{0}\Big)\gamma^+ q\Big(\frac{x^-}{2},0,\mathbf{0}\Big)|N\rangle\\ &= \overline{u}_{N'}\gamma^+ u_N \int dx\, H(x,\xi,t) \,+\, \overline{u}_{N'}\frac{i\sigma^{+\nu}q_\nu}{2M}u_N \int dx\, E(x,\xi,t)\,. \end{aligned} \tag{4}$$

The new objects $H(x,\xi,t)$ and $E(x,\xi,t)$ are called Generalized Parton Distributions (GPDs), because they do not only depend on the "longitudinal" LC momentum fraction x of partons, but also on the skewness $\xi = (P-P')^+/(P+P')^+$, which describes the change in the "longitudinal" LC momentum of the nucleon, as well as on $t = (P'-P)^2$. GPDs allow for a unified description of several hadronic properties [6]: from equation (4) their integral in x yields the nucleon electromagnetic form factors; while the so-called forward limit, $\xi, t \to 0$, reduces them to the conventional Parton Distribution Functions (PDFs). GPDs emerge in any DIS process with production of real photons (Deeply-Virtual Compton Scattering, DVCS) or of mesons (Deeply-Virtual Meson Production, DVMP), because corresponding factorization theorems hold at any order in α_s when $Q^2 \gg t$ [7]. Consequently, GPDs depend also on the hard scale Q^2 of the process at which they are extracted. For simplicity, this dependence will be omitted in the following, unless explicitly mentioned.

2.1. GPDs and impact parameter densities

The connection between GPDs and the spatial structure of the nucleon can be made evident by using nucleon states that are transversally localized in space. In fact, in IMF the boosts along transverse directions do not depend on interactions and form a kinematic subgroup of the Poincaré group that obeys the same commutation relations as in ordinary nonrelativistic quantum mechanics. The nucleon state with transverse c.m. $\boldsymbol{R} = 0$ is built by [8]

$$|N(P^+,\boldsymbol{R}=0,S)\rangle = \mathcal{N}\int \frac{d\boldsymbol{P}_T}{(2\pi)^2}\,|N(P^+,\boldsymbol{P}_T,S)\rangle\,, \tag{5}$$

where $\mathcal{N}$ is a suitable normalization and the integral is limited to $|\boldsymbol{P}_T| \ll P^+$ in order to preserve the partonic interpretation. Having defined states at $\boldsymbol{R} = 0$, it is possible to define also transverse distances $\boldsymbol{b}$ with respect to $\boldsymbol{R}$, then to make a translation by $\boldsymbol{b}$ in the operator appearing in equation (4), and finally to define the impact-parameter dependent distribution [4]

$$\begin{aligned} q(x,\boldsymbol{b}) &= \int \frac{dx^-}{2\pi}\, e^{ixP^+x^-}\, \langle N(P^+,\boldsymbol{R}=0,S)|\overline{q}\Big(-\frac{x^-}{2},0,\boldsymbol{b}\Big)\gamma^+ q\Big(\frac{x^-}{2},0,\boldsymbol{b}\Big)|N(P^+,\boldsymbol{R}=0,S)\rangle\\ &= |\mathcal{N}|^2\int \frac{d\boldsymbol{P}'_T}{(2\pi)^2}\frac{d\boldsymbol{P}_T}{(2\pi)^2}\, e^{i(\boldsymbol{P}'_T-\boldsymbol{P}_T)\cdot\boldsymbol{b}}\int \frac{dx^-}{2\pi}\, e^{ixP^+x^-}\\ &\qquad\qquad \times\langle N(P^+,\boldsymbol{P}'_T,S)|\overline{q}\Big(-\frac{x^-}{2},0,\mathbf{0}\Big)\gamma^+ q\Big(\frac{x^-}{2},0,\mathbf{0}\Big)|N(P^+,\boldsymbol{P}_T,S)\rangle\\ &= \int \frac{d\boldsymbol{q}}{(2\pi)^2}\, e^{i\boldsymbol{q}\cdot\boldsymbol{b}}\, H(x,\xi=0,t=-\boldsymbol{q}^2)\,. \end{aligned} \tag{6}$$

That $q(x,\boldsymbol{b})$ is a partonic density, it can be recognized by taking the integral over x:

$$\begin{aligned} q(\boldsymbol{b}) &= \int dx\, q(x,\boldsymbol{b}) = \langle N(P^+,\boldsymbol{R}=0,S)|q^\dagger_+(0,0,\boldsymbol{b})\, q_+(0,0,\boldsymbol{b})\,|N(P^+,\boldsymbol{R}=0,S)\rangle\\ &= \int \frac{d\boldsymbol{q}}{(2\pi)^2}\, e^{i\boldsymbol{q}\cdot\boldsymbol{b}}\, F_1(Q^2=\boldsymbol{q}^2)\,, \end{aligned} \tag{7}$$

and by recalling that $\bar{q}\gamma^+ q = \sqrt{2} q_+^\dagger q_+$, where $q_+ = P_+ q$ is the LC "good" component of the partonic field q, with $P_+ = 1/2\,\gamma^-\gamma^+$.

Therefore, by taking the specific limit $\xi = 0, t = -(\boldsymbol{P}'_T - \boldsymbol{P}_T)^2$, namely by letting the nucleon change only its transverse momentum while keeping the same P^+, the Fourier transform of the nonspin-flip GPD H gives the impact-parameter dependent distribution $q(x, \boldsymbol{b})$, which describes the probability density for a parton with flavor q and LC momentum x to be located in the transverse plane at distance $\boldsymbol{b}$ from the transverse c.m. $\boldsymbol{R} = 0$. Hence, for each x we can take a snapshot of the nucleon in the transverse plane: we can make a nucleon tomography.

Equation (7) gives a solution to the puzzle depicted at the end of section 1: the Fourier transform of the Dirac form factor F_1 gives access to the nucleon charge distribution in the transverse plane when the nucleon is moving relativistically with large LC "longitudinal" momentum in the IMF.

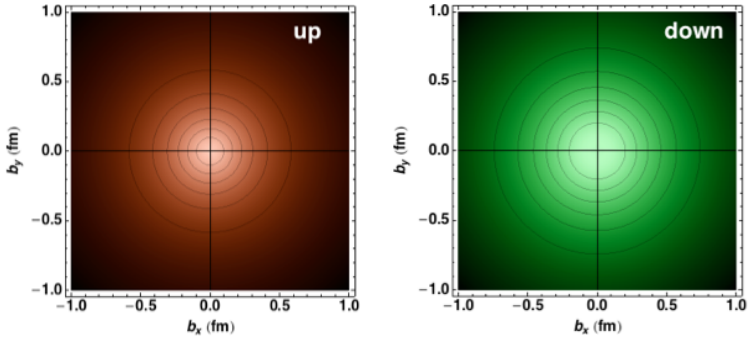

(a) (b)

Figure 1. (Color online) The charge distribution of up quark (a) and down quark (b) in the transverse plane, as obtained by Fourier transforming the Dirac form factor parametrized in Ref. [9]. Figure adapted from Ref. [10].

In figure 1, the plot for the up (a) and down (b) transverse charge distributions $q(\boldsymbol{b})$ are shown, as obtained by taking the parametrization of F_1 from Ref. [9]. We can remark that the down quark appears wider than the up by almost 30%. Interestingly, if the same exercise is repeated for the neutron, the resulting profile of $q(|\boldsymbol{b}|)$ shows that the central core is negatively charged while the peripheral cloud (supposedly made of pions) is positively charged [8], contrary to naïve expectations based on the idea that the neutron is somewhat a proton surrounded by a negatively charged pion cloud.

2.2. Polarized nucleons

In equation (6), the matrix elements do not involve the flip of the nucleon helicity S. For a transversely polarized N, e.g., along $\hat{y}$, the polarization state is $|N(P, S_y)\rangle = (|N(P, S)\rangle + i|N(P, -S)\rangle)/\sqrt{2}$. Hence, the more general version of equation (6) for a transversely polarized N involves both nonspin-flip and spin-flip matrix elements, therefore it involves both the GPDs H and E. Following the same pattern leading to equation (7), it is easy to realize that the Fourier transform of the GPD E in the limit $\xi = 0, t = -\boldsymbol{q}^2$, introduces a distortion in the transverse charge density related to the Pauli form factor. In formulae, the final expression of the transverse charge density reads [11]

$$\rho(\boldsymbol{b}) = q(\boldsymbol{b}) + \cos\phi_b \int \frac{dQ}{2\pi} \frac{Q^2}{2M} J_1(Q|\boldsymbol{b}|)\, F_2(Q^2 = \boldsymbol{q}^2)\ . \tag{8}$$

We deduce that the transverse polarization of the nucleon along $\hat{y}$ produces a distortion of its transverse charge density along $\hat{x}$ (since $\boldsymbol{b} = |\boldsymbol{b}|\{\cos\phi_b, \sin\phi_b\}$), and the size of the effect is proportional to its anomalous magnetic moment $\kappa = F_2(0)$. In figure 2, we show this effect as obtained by taking again the parametrization of F_1 and F_2 from Ref. [9]. A natural explanation

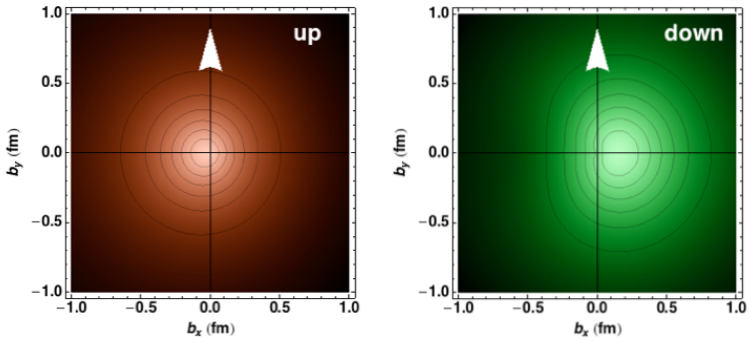

(a) (b)

Figure 2. (Color online) The distorted charge distribution of up quark (a) and down quark (b) in the transverse plane for a proton transversely polarized along $\hat{y}$, as obtained by Fourier transforming the Dirac and Pauli form factors parametrized in Ref. [9]. Figure adapted from Ref. [10].

is that a spin-orbit effect is active at the partonic level. So one may wonder if GPDs can open the doorway to explore the still unsolved puzzle about the partonic decomposition of the N spin.

3. GPDs and the N spin

Equation (4) can be generalized to calculating the nucleon matrix elements of the "m-spin" operator $\hat{O}^{\mu}_{\mu_1...\mu_m} = \overline{q}(0)\gamma^{\mu} i D^{\leftrightarrow}_{\mu_1} ... i D^{\leftrightarrow}_{\mu_m} q(0)$ [6],

$$\begin{aligned}\langle N'|\hat{n}^{\mu_1}...\hat{n}^{\mu_m}\hat{O}^{\mu}_{\mu_1...\mu_m}|N\rangle &= \overline{u}_{N'}\gamma^{\mu}u_N \sum_{i\,\mathrm{even}}^{m} A_{m+1,i}(t)\,(2\xi)^i + \overline{u}_{N'}\frac{i\sigma^{\mu\nu}q_\nu}{2M}u_N \sum_{i\,\mathrm{even}}^{m} B_{m+1,i}(t)\,(2\xi)^i \\ &= \overline{u}_{N'}\gamma^{\mu}u_N \int dx\, x^m\, H(x,\xi,t) \;+\; \overline{u}_{N'}\frac{i\sigma^{\mu\nu}q_\nu}{2M}u_N \int dx\, x^m\, E(x,\xi,t)\;, \end{aligned} \tag{9}$$

where the light-like 4-vectors $\hat{n}^{\mu_1}, ..., \hat{n}^{\mu_m}$, are chosen to satisfy $\hat{n}\cdot(P+P')/2 = 1$ and $\hat{n}\cdot q = -2\xi$. Equation (9) illustrates the so-called polinomiality of GPDs, namely the fact that their m-th Mellin moment in x can be represented as an even polynomial in ξ. The polynomial coefficients $A_{m+1,i}(t)$, $B_{m+1,i}(t)$, are named Generalized Form Factors (GFFs); we have $A_{1,0}(t) \equiv F_1(t)$ and $B_{1,0}(t) \equiv F_2(t)$.

Starting from the energy-momentum density tensor of QCD, we can define the angular momentum operator $\hat{J}^f_i$ for a parton of flavor f, and expand its nucleon matrix elements by specializing equation (9) to $m = 1$ such that

$$\begin{aligned}\frac{1}{2} &= \sum_{f=q,\overline{q},g} J^f_z \equiv \sum_{f=q,\overline{q},g} \langle N(P,S=1/2)|\hat{J}^f_z|N(P,S=1/2)\rangle \\ &= \frac{1}{2}\sum_{f=q,\overline{q},g}\Big[A^f_{2,0}(0) + B^f_{2,0}(0)\Big] = \frac{1}{2}\int_0^1 dx\, x\,\Big[H^f(x,0,0) + E^f(x,0,0)\Big]\;. \end{aligned} \tag{10}$$

The last line of equation (10) represents the so-called Ji's sum rule [6] and illustrates the connection between GPDs and the problem of decomposing the N spin in terms of its elementary constituents. On the other hand, the Ji's sum rule sets a challenge to practical calculations of J^f_z. The forward limit $\xi, t \to 0$, of the nonspin-flip GPD H^f is simply the well known unpolarized PDF $f^f_1(x)$ (or the $q(x)$ recovered by integrating the impact parameter $\boldsymbol{b}$ in equation (6)). But the forward limit of the spin-flip GPD E^f is not accessible, because in this limit there is no handle to describe the N spin flip. So, any calculation of J^f_z based on the extraction of GPDs from, e.g. DVCS/DVMP data, needs a model-dependent extrapolation to reach the forward

limit of E. Moreover, in equation (10) it is understood that any partonic object depends also on Q^2: the GPDs do explicitly depend on the hard scale of the process at which they are extracted (see section 2); hence, also the contribution to the total angular momentum by each specific flavor does. The balance between the different flavors is ruled by evolution equations of DGLAP type [12], because the Mellin moments in x do not alter the short-distance behaviour of QCD. In the asymptotic limit $Q^2 \to \infty$ of the IMF, the N spin is shared approximately in equal parts by (anti)quarks and gluons (for $n_f = 5$ flavors).

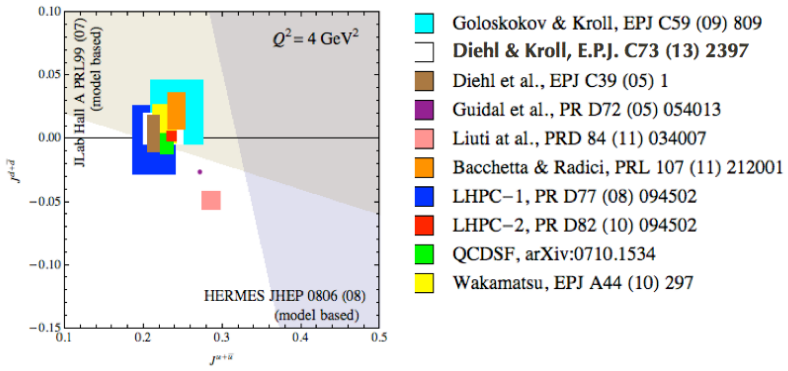

Figure 3. (Color online) The contribution to the N spin carried by $d + \overline{d}$ against $u + \overline{u}$ at $Q^2 = 4$ GeV^2. From top down, the first five boxes refer to the extraction of GPDs from exclusive DVCS data. The 6$^{\text{th}}$ box refers to the connection between GPD E and TMD $f_{1T}^{\perp}$. The last four boxes refer to calculations of GFFs on lattice. Figure adapted from Ref. [13].

In figure 3, the contribution to the N spin carried by the total angular momentum of the $d + \overline{d}$ flavor is plotted against the $u + \overline{u}$ one at the scale $Q^2 = 4$ GeV^2 (figure adapted from Ref. [13]). The notation is the following. From top down, the first five boxes refer to the calculation of the Ji's sum rule (10) based on the extraction of GPDs H and E from exclusive DVCS data. The result corresponding to the 6$^{\text{th}}$ box will be described in section 4. The last four boxes describe some of the results obtained on lattice, where the GFFs in equation (10) can be directly computed. From figure 3, we deduce that almost all calculations are compatible within errors. There is a general consensus about the fact that quarks and antiquarks carry together slightly more than half of the N spin (at the indicated scale), and that 85% of this portion is carried by the flavor u. The sea quark contribution is smaller by one order of magnitude, but the uncertainty in the calculation is still very large. Nothing is known about the gluon contribution, except that experimental measurements with polarized nucleons indicate an almost vanishing gluon helicity [14] (but with large errors).

3.1. The Orbital Angular Momentum of partons

At the end of section 2.2, we stated that the observed distortion of the transverse charge distribution of partons in transversely polarized nucleons must be attributed to a sort of spin-orbit effect generated by the orbital motion of partons. But the Ji's sum rule (10) gives access only to the total angular momentum carried by partons. So, it comes natural to wonder if GPDs are useful tools to deduce information also on the Orbital Angular Momentum (OAM) of partons.

By inspecting the analytic structure of the partonic total angular momentum that can be deduced from the QCD energy-momentum tensor, it is natural to define the OAM L_z^f for a parton with flavor f as the difference between its total angular momentum J_z^f and its helicity S_z^f. Using equation (10), we can identify it as the Mellin moment of the OAM distribution

function $L_z^f(x)$ defined as [12]

$$L_z^f = J_z^f - S_z^f = \int_0^1 dx\, L_z^f(x) = \frac{1}{2}\int_0^1 dx \left\{ x \left[f_1^f(x) + E^f(x,0,0) \right] - g_1^f(x) \right\}, \qquad (11)$$

where $g_1^f(x)$ is the well known helicity distribution for a flavor f (at the hard scale Q^2).

The definition (11) is gauge invariant, but above all it defines a measurable quantity: f_1 and g_1 are extracted from inclusive DIS of electrons on (polarized) nucleons, while E can be extracted from exclusive DVCS or DVMP. Unfortunately, the analytic structure of the QCD energy-momentum tensor does not allow to decompose the gluon total angular momentum in a similar manner. Moreover, the operator defined through equation (11) does not satisfy the canonical commutation relations of a general angular momentum operator. In the literature, another definition of $\hat{J}^f$ [15] appeared before the one in equation (10). It allows for a clear decomposition of both quark and gluon parts into the respective OAM and helicity contributions, each term defining an operator that satisfies the canonical commutation relations. However, this so-called Jaffe-Manohar decomposition is not gauge invariant. Several attempts to extend it to a gauge invariant quantity have been released. The discussion is still open about which choice is more convenient (for a recent review, see Ref. [16]).

An alternative definition of OAM can be built in terms of the so-called Wigner distributions $W_{S,S_q}(x, \boldsymbol{p}_T, \boldsymbol{b})$, which contain information on the correlation between the transverse momentum $\boldsymbol{p}_T$ and position $\boldsymbol{b}$ of a parton with helicity S_q and LC "longitudinal" fraction x of the momentum of the parent nucleon with helicity S [17]. The 5-dimensional W contain the maximum information about the dynamics of partons inside the nucleon moving in the IMF. By construction, they are not positive-definite, i.e. they are not densities. But they are not constrained by the Heisenberg principle because $\boldsymbol{p}_T$ is not the conjugate variable of $\boldsymbol{b}$. The impact-parameter distribution $q(x, \boldsymbol{b})$ of equation (6) can be recovered from the Wigner distribution $W(x, \boldsymbol{p}_T, \boldsymbol{b})$ by simply integrating its $\boldsymbol{p}_T$ dependence. For an unpolarized quark in a longitudinally polarized nucleon, the quark OAM can be defined as [18]

$$l_z^q = \int d\boldsymbol{b} \left[\boldsymbol{b} \times \int dx\, d\boldsymbol{p}_T\, \boldsymbol{p}_T\, W_{LU}^q(x, \boldsymbol{p}_T, \boldsymbol{b}) \right]_z = \int d\boldsymbol{b} \left[\boldsymbol{b} \times \langle \boldsymbol{p}_T^q \rangle(\boldsymbol{b}) \right]_z . \qquad (12)$$

In the above definition, the W's are used as semi-classical phase space distributions to define the average transverse momentum $\langle \boldsymbol{p}_T^q \rangle(\boldsymbol{b})$ carried by a quark q in a certain transverse position $\boldsymbol{b}$. The OAM is then built by generalizing the classical definition. The l_z^q operator satisfies the canonical commutation relations but it is built with objects, the Wigner distributions, that cannot be extracted from any known process. Anyway, the definition (12) can be used to test models of the Wigner distribution, i.e. of the N wave function.

The definition (11) is undoubtedly more convenient also because L_z^f can be calculated on the lattice. Most lattice calculations, some of which are reported in figure 3, converge to the result that $L_z^u \approx 0.3 \sim -L_z^d$. The helicities S_z^f of quarks $f = u, d, s$, are constrained to add up to the nucleon singlet axial charge g_A^0. The lattice result for g_A^0 is rather close to its experimental value and implies that quark helicities contribute at most to 25% of the N spin, i.e. they amount to ≈ 0.125. Since the extracted gluon helicity is approximately almost vanishing and nothing is basically known about the gluon OAM, the strong cancellation of quark OAM leaves the puzzle about the N spin decomposition still open.

4. The Transverse-Momentum Distributions

In the previous section, we introduced the Wigner distributions $W_{S,S_q}(x, \boldsymbol{p}_T, \boldsymbol{b})$, that contain the most complete information on the parton dynamics inside a nucleon moving in the IMF. Even if

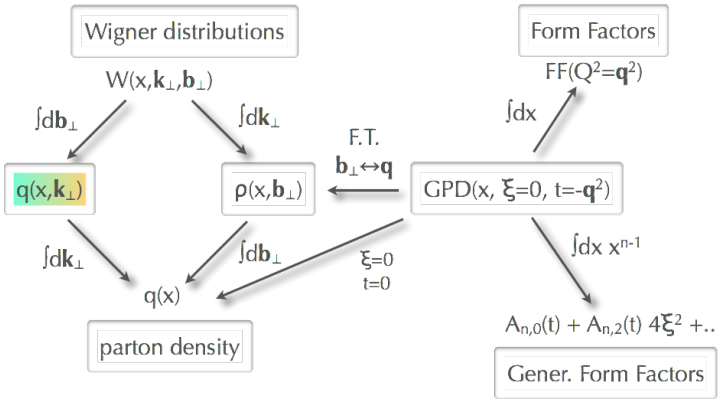

Figure 4. The roadmap to a multi-dimensional exploration of the N inner structure. The marked box shows the role of TMDs in completing the manifold picture starting from the Wigner distributions W's down to the usual parton densities PDFs (adapted from Ref. [19]).

the definition is somewhat academic because no process is currently known where the W's could be extracted from, it has been pointed out that by simply integrating the $\boldsymbol{p}_T$ dependence for an unpolarized parton we can recover the impact-parameter distribution $q(x, \boldsymbol{b})$ of equation (6), which is actually measurable through the bidimensional Fourier transform of the Dirac and Pauli form factors. Analogously, it is natural to explore the consequence of integrating the $\boldsymbol{b}$ dependence of the W's. In this way, we can build new partonic densities in momentum space, the Transverse-Momentum Distributions $q(x, \boldsymbol{p}_T)$ (TMDs), that describe the probability density of finding a parton with flavor q and polarization S_q carrying a LC "longitudinal" momentum x and a transverse momentum $\boldsymbol{p}_T$. Since the impact parameter $\boldsymbol{b}$ is the conjugate variable of $\boldsymbol{q} = \boldsymbol{P}'_T - \boldsymbol{P}_T$ and not of $\boldsymbol{p}_T$, the TMDs are not simply the Fourier transforms of $q(x, \boldsymbol{b})$. Lastly, by integrating the $\boldsymbol{p}_T$ dependence of TMDs we recover the standard PDFs as functions of x. Hence, the TMDs contain a more detailed information on the dynamics of partons in momentum space and represent a new milestone in the roadmap to the exploration of the nucleon internal structure (see figure 4).

quark pol.

nucleon pol.	U	L	T
U	f_1		$h_1^\perp$
L		g_{1L}	$h_{1L}^\perp$
T	$f_{1T}^\perp$	g_{1T}	h_1, $h_{1T}^\perp$

Twist-2 TMDs

Figure 5. The eight leading-twist TMDs organized according to the unpolarized (U), longitudinal (L), or transverse (T) polarization state of the parton (along table rows), or of the parent nucleon (along table columns).

At leading twist, there are eight TMDs. They are grouped in figure 5 according to the unpolarized (U), longitudinal (L), or transverse (T) polarization state of the parton (along the table rows) or of the parent nucleon (along the table columns). The TMDs can be typically extracted in Semi-Inclusive processes in the DIS regime (SIDIS) where one measures the azimuthal angle of the final-state products around a reference axis defined in the lab frame. If the transverse momentum of the outgoing particles is small with respect to the hard scale Q of the process, a specific factorization proof has been put forward [20]. In this framework, the cross section can be parametrized in terms of various structure functions (depending on the polarization of the beam/target/final products), each one involving a specific TMD in the table of figure 5 (and a corresponding fragmentation function, if the detected final products are hadrons) [21]. Each structure function has a peculiar dependence upon the azimuthal angle of the final products, as well as the azimuthal angle of the various polarization vectors involved. Consequently, it can be isolated through azimuthal asymmetries, sometimes involving a spin

flip of a polarized particle (in which case, we deal with Single-Spin Asymmetries - SSAs). Several experimental measurements of azimuthal asymmetries were performed in the last 15 years, addressing each one of the eight TMDs in figure 5. However, the collected amount of data is not yet sufficient to grant a knowledge of TMDs comparable to what we have learnt so far about PDFs. Only recently first attempts to parametrize the unpolarized $f_1^q(x, \boldsymbol{p}_T)$ have appeared in the literature [22, 23], in order to explore if and how the $\boldsymbol{p}_T$ dependence changes with flavor q and with x.

On the other hand, the literature about theoretical investigations on TMDs is vast and the discussion is still open about setting up the proper framework for describing their evolution with the hard scale (see Refs. [21, 24] and references therein, for a comprehensive review). Here, we just mention two elements in figure 5 that historically triggered the focus on this field.

The first one is the function h_1 appearing in the lower right corner of the table. It describes the unbalance between number densities of partons with transverse polarization parallel or antiparalllel to the transverse polarization of the parent nucleon. As such, it is connected to elementary mechanisms flipping the parton helicity; in jargon, it is named transversity and referred to as a chiral-odd distribution. If we integrate the $\boldsymbol{p}_T$ dependence of TMDs, all the entries in the table of figure 5 disappear except for the three elements in the diagonal: $f_1(x)$, $g_{1L}(x) \equiv g_1(x)$, and just $h_1(x)$. All three PDFs are necessary to reach a complete partonic picture of the N (spin) structure at leading twist. But the momentum and helicity distributions are usually extracted from inclusive DIS processes, while the transversity is suppressed because it is a chiral-odd function. The h_1 can be extracted only in semi-inclusive processes involving another chiral-odd partner. The typical example, for which there are experimental data, is the SIDIS on transversely polarized protons. If a single pion is detected and its azimuthal distribution is measured, the h_1 gets convoluted with a chiral-odd fragmentation function that relates the transverse polarization of the (fragmenting) quark to the transverse momentum of the final pion, the so-called Collins function [25]. In this way, the $h_1^u(x)$ and $h_1^d(x)$ were extracted for the first time (for more details on the most updated result, see Ref. [26]). If two pions are detected with a small transverse relative momentum $|\boldsymbol{R}_T| \ll Q$ and in a collinear kinematics (i.e., with a vanishing transverse component of their total momentum), the $h_1(x)$ is simply multiplied by the di-hadron fragmentation function $H_1^{\sphericalangle}$ that relates the transverse polarization of the fragmenting quark to $\boldsymbol{R}_T$ [27, 28, 29, 30]. The advantage of this method is that the collinear framework remarkably simplifies the theoretical description. Recent experimental data for the detection of $(\pi^+\pi^-)$ pairs allowed for a direct extraction of the valence contributions to the proton $h_1(x)$ [31, 32]. Within the experimental statistical errors, this extraction is compatible with the one based on the Collins effect. This is a remarkable achievement because it opens the doorway to a more precise determination of the theoretically interesting, but yet poorly known, tensor charge, i.e. the first Mellin moment of $h_1(x)$.

The second element in figure 5, that historically drew the interest in TMDs, appears in the lower left corner of the table. It describes the difference in the momentum distribution of unpolarized partons when in IMF they move together inside a parent nucleon with transverse polarization parallel or antiparallel to a specific transverse direction [33]. For many years, this function has been thought to vanish because of time-reversal symmetry; in jargon, it is classified as a naïve T-odd function [1]. Nevertheless, it addresses the same physics of the impact-parameter distribution $\rho(\boldsymbol{b})$ in equation (8), but in momentum space. Therefore, it must have a close connection to the problem of the partonic decomposition of the N spin.

[1] There are two naïve T-odd distributions in the table of figure 5 of leading-twist TMDs: the Sivers function $f_{1T}^{\perp}$ and its "mirror" $h_1^{\perp}$, the Boer-Mulders function, that in an unpolarized hadron describes the unbalance between partons transversely polarized along or against a specified transverse direction.

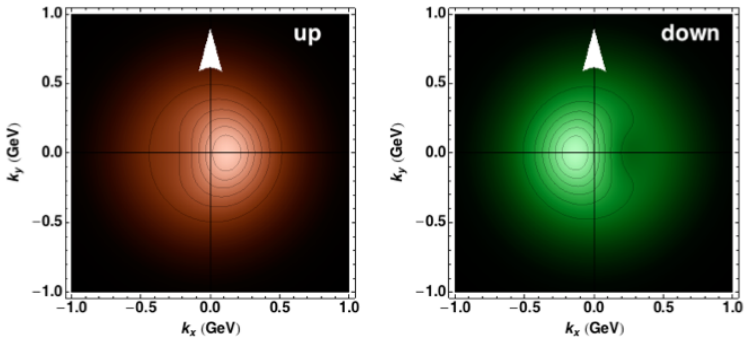

(a) (b)

Figure 6. (Color online) The distorted momentum distribution of up quark (a) and down quark (b) in the transverse plane for a proton transversely polarized along $\hat{y}$, as obtained by parametrizing the Sivers effect [10].

4.1. The Sivers function and the N spin

In figure 6, the left panel shows the distortion of the momentum distribution of the up quark in the transverse plane when the parent proton is transversely polarized along $\hat{y}$ (indicated by the white arrow) and moves towards the reader. The right panel shows an opposite distortion for the down quark. The distortion is clearly along $\hat{x}$: the effect is similar to the one depicted in figure 2 but in momentum space, and its size is given by the Sivers function $f_{1T}^{\perp}$ [10]. Therefore, we can argue that the quarks drift in opposite directions, according to their charge, because also in this case they are subjected to a sort of spin-orbit effect. The Sivers function appears in the cross section for the same process as the Collins effect, namely the SIDIS off transversely polarized protons leading to the detection of a single pion. However, it is contained in a structure function with a different dependence on the azimuthal angles of the final pion and of the proton target polarization. Hence, it can be isolated through a different SSA, the so-called Sivers effect. Sensitive to the distortion induced by spin-orbit, the unpolarized struck parton eventually fragments into the detected pion with an azimuthally asymmetric distribution. The Sivers effect has been measured by three different collaborations: HERMES at DESY [34], COMPASS at CERN [35], and Hall A at Jefferson Lab [36]. Several parametrizations have been figured out to extract the x dependence of the Sivers function from these data. Most of them agree that the valence up and down contributions have similar size but opposite sign, the $f_{1T}^{\perp u}$ being negative [37, 38]. The distortions displayed in figure 6 are a direct consequence of these results. The contribution of the sea quarks is much more questionable, because the statistical errors are large and the size presumably very small [38]. Many theoretical papers have recently appeared also on the development of evolution equations for the Sivers function in the TMD framework. The topic is matter of intense debate and entering the details is beyond the scope of this presentation.

Since the Sivers effect originates from a spin-orbit distortion of the motion of partons, it is natural to suspect that it can play a role in the partonic decomposition of the N spin. The starting point is the Ji's sum rule (10) described in section 3. We already stressed that the forward limit of the spin-flip GPD $E(x, 0, 0)$ cannot be accessed, forcing to model-dependent extrapolations. However, we already noted that both the GPD E and the TMD $f_{1T}^{\perp}$ describe from two different perspectives the distortion induced by the same fact, namely that the nucleon is transversely polarized. It is natural to try to establish a link between the two pictures. But one effect is not the Fourier transform of the other: the impact parameter $\boldsymbol{b}$ is conjugate to the nucleon transverse momentum change $\boldsymbol{P}_T' - \boldsymbol{P}_T = \boldsymbol{q}$, not to the parton transverse momentum $\boldsymbol{p}_T$. A rigorous derivation of this link is very difficult, because it would imply a description of the nonperturbative color forces exerted on the active parton by the surrounding spectators. A semi-classical interpretation is possible, it is referred to as the "color lensing" effect [39] and it is described in figure 7.

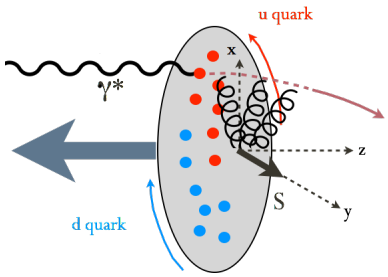

Figure 7. The color lensing effect [39].

In the Sivers effect, in the c.m. frame the nucleon is moving along the longitudinal direction against the virtual photon probe γ^*. The nucleon is transversely polarized along $\hat{y}$ with polarization S. Consequently, the charge distribution of partons is distorted along $\hat{x}$ because of a spin-orbit effect induced by the GPD E: the up quarks accumulate in the $x > 0$ hemisphere rotating anti-clockwise, and viceversa for the down quarks. When the virtual photon probe hits an up quark, it will preferably do it in the $x > 0$ hemisphere. In the DIS regime, the momentum transfer absorbed is very large and the struck quark tries to escape the nucleon. The attractive color forces deflect the trajectory of the up quark towards the $x < 0$ hemisphere. Confinement implies that the up quark eventually fragments into a π^+, preferably detected in the $x < 0$ hemisphere. Analogously, a π^- emerging from the fragmentation of a down quark would be preferably detected in the $x > 0$ hemisphere. This asymmetric distribution of pions along $\hat{x}$ is reminiscent of the distortion of quark distributions in momentum space described by the Sivers function $f_{1T}^{\perp}$. According to this semi-classical picture, the GPD E and the TMD $f_{1T}^{\perp}$ are connected by a complicated analytical formula that involves a function describing the above mentioned residual color forces [39]. Hence, an actual calculation of the color lensing effect requires model assumptions. Inspired by the spectator diquark model [40], at some scale Q_L we used the relation [38]:

$$f_{1T}^{\perp\,(0)f}(x;Q_L^2) = -L(x)\,E^f(x,0,0;Q_L^2)\,, \tag{13}$$

in order to compute the parton total angular momentum through the Ji's sum rule by using the parametrization of the x dependence of the Sivers function obtained from SIDIS data on the Sivers effect, and by constraining its integral to reproduce the N anomalous magnetic moment. In equation (13), the left hand side represents the first moment in $\boldsymbol{p}_T$ of the Sivers function $f_{1T}^{\perp\,f}(x,\boldsymbol{p}_T;Q_L^2)$. The total angular momenta obtained with this procedure produce the results identified by the 6$^{\text{th}}$ box (from top down) in the column of references displayed on the right of figure 3, in good agreement with the results obtained by very different procedures (see section 3).

The color lensing effect of equation (13) suggests that the content of the Sivers function $f_{1T}^{\perp}$ crucially depends on the structure of the residual color forces felt by the struck parton. In the SIDIS process of figure 7, these color forces represent a sort of "final-state interaction" effect. But $f_{1T}^{\perp}$ can appear also in other hard processes involving transversely polarized nucleons like, e.g., the hadronic collision leading to the semi-inclusive production of Drell-Yan lepton pairs. If one of the two colliding hadrons is a transversely polarized nucleon, the Sivers effect is now realized by producing a virtual photon with a transverse momentum with respect to the average collision direction and, eventually, by producing an azimuthally asymmetric distribution of the final lepton pair. However, in the hadronic collision the annihilating quark coming from the transversely polarized nucleon feels the color field generated inside the other colliding hadron as if, intuitively, it were a sort of "initial-state interaction". By a careful inspection of the color structure of the involved nonlocal operator, the net effect is that the Sivers function should appear with an opposite sign with respect to the SIDIS cross section, thus breaking in principle its universality feature [41]. Since experimental data for semi-polarized Drell-Yan processes are

not yet available, this result is a true prediction based on the general nonperturbative color structure dictated by QCD gauge invariance. Hence, an experimental test of this prediction is of outmost importance [42, 19].

References

[1] Mueller B 2005 *Nucl. Phys. A* **750** 84
[2] Miller G A 2009 *Phys. Rev. C* **80** 045210
[3] Miller G A 2010 *Ann. Rev. Nucl. Part. Sci.* **60** 1
[4] Burkardt M 2003 *Int. J. Mod. Phys. A* **18** 173
[5] Diehl M 2002 *Eur. Phys. J. C* **25** 223
[6] Ji X 1997 *Phys. Rev. Lett.* **78** 610
[7] Collins J C and Freund A 1999 *Phys. Rev. D* **59** 074009
[8] Miller G A 2007 *Phys. Rev. Lett.* **99** 112001
[9] Kelly J 2004 *Phys. Rev. C* **70** 068202
[10] Bacchetta A and Contalbrigo M 2012 *Il Nuovo Saggiatore* **28** 16
[11] Carlson C E and Vanderhaeghen M 2008 *Phys. Rev. Lett.* **100** 032004
[12] Hoodbhoy P, Ji X D, and Lu W 1999 *Phys. Rev. D* **59** 014013
[13] Bacchetta A and Radici M 2012 *PoS* **QNP2012** 041
[14] Aschenauer E *et al.* 2013 `arXiv:1304.0079`
[15] Jaffe R L and Manohar A 1990 *Nucl. Phys. B* **337** 509
[16] Leader E and Lorce C 2013 `arXiV:1309.4235`
[17] Lorce C, Pasquini B, and Vanderhaeghen M 2011 *JHEP* **1105** 041
[18] Lorce C, Pasquini B, Xiong X, and Yuan F 2012 *Phys. Rev. D* **85** 114006
[19] Accardi A *et al.* 2012 `arXiv:1212.1701`
[20] Ji X, Ma J P, and Yuan F 2004 *Phys. Lett. B* **597** 299
[21] Bacchetta A, Diehl M, Goeke K, Metz A, Mulders P J, and Schlegel M 2007 *JHEP* **02** 093
[22] Signori A, Bacchetta A, Radici M, and Schnell G 2013 *JHEP* **1311** 194
[23] Anselmino M, Boglione M, J O Gonzales H, Melis S, and Prokudin A 2014 *JHEP* **1404** 005
[24] Collins J 2011 *Foundations of Perturbative QCD* (Cambridge University Press)
[25] Collins J C 1993 *Nucl. Phys. B* **396** 161
[26] Anselmino M *et al.* 2013 *Phys. Rev. D* **87** 094019
[27] Collins J C and Ladinsky G A 1994 `arXiv:hep-ph/9411444`
[28] Jaffe R L, Jin X, and Tang J 1998 *Phys. Rev. Lett.* **80** 1166
[29] Radici M, Jakob R, and Bianconi A 2002 *Phys. Rev. D* **65** 074031
[30] Bacchetta A and Radici M 2003 *Phys. Rev. D* **67** 094002
[31] Bacchetta A, Courtoy A, and Radici M 2011 *Phys. Rev. Lett.* **107** 012001
[32] Bacchetta A, Courtoy A, and Radici M 2013 *JHEP* **1303** 119
[33] Sivers D W 1990 *Phys. Rev. D* **41** 83
[34] Airapetian A *et al.* (The HERMES Collaboration) 2009 *Phys. Rev. Lett.* **103** 152002
[35] Alekseev M *et al.* (The COMPASS Collaboration) 2009 *Phys. Lett. B* **673** 127
[36] Qian X *et al.* (The Jefferson Lab Hall A Collaboration) 2011 *Phys. Rev. Lett.* **107** 072003
[37] Anselmino M, Boglione M, and Melis S 2012 *Phys. Rev. D* **86** 014028
[38] Bacchetta A and Radici M 2011 *Phys. Rev. Lett.* **107** 212001
[39] Burkardt M 2002 *Phys. Rev. D* **66** 114005
[40] Bacchetta A, Conti F, and Radici M 2008 *Phys. Rev. D* **78** 074010
[41] Collins J C 2002 *Phys. Lett. B* **536** 43
[42] Denisov O (The COMPASS Collaboration) 2012 *Nuovo Cim. C* **035N2** 239